GLOBAL MODES CONSTITUTING THE SOLAR MAGNETIC CYCLE

III. *'Shapes' and 'Sizes' of the Sunspot Cycles and Maintenance of MHD Spectrum by Energy Cascade*

M. H. GOKHALE and J. JAVARAIAH
Indian Institute of Astrophysics, Bangalore 560 034, India

(Received 8 February, 1994; in revised form 12 September, 1994)

Abstract. The 'sunspot occurrence probability' defined in Paper I is used to determine the Legendre–Fourier (LF) terms in the 'rate of emergence of toroidal magnetic flux, $Q(\theta, t)$, above the photosphere per unit latitude interval, per unit time'. Assuming that the magnetic flux tubes whose emergence yields solar activity are produced by interference of global MHD waves in the Sun, we determine how the amplitudes and phases of the LF terms in the toroidal magnetic field B_Φ, representing the waves, will be related to those of the LF terms in $Q(\theta, t)$. The set of LF terms in 'Q' that represents the set of waves whose interference produces most of the observed sunspot activity is $\{l = 1, 3, \ldots, 13; \nu = n\nu_*, n = 1, 3, 5\}$, where $\nu_* = 1/21.4$ yr^{-1}. However, among the 'shapes' of sunspot cycles modeled using various sets of the computed LF terms the best agreement with the observed shape, for each cycle, is given by the set $\{l = 3$ or $l = 3, 5$; and $n = 1, 3$ or $n = 1, 3, 5\}$. The sets of terms: $\{l = 1, 3, 5, 7; n = 1\}$, $\{l = 1, 3, 5, 7; n = 3\}$, $\{l = 9, 11, 13, 15; n = 1\}$ and $\{l = 9, 11, 13, 15; n = 3\}$ seem to represent four modes of global MHD oscillation. Correlations between the amplitudes (and phases) of LF terms in different modes suggest possible existence of cascade of energy from constituent MHD waves of lower l and n to those of higher l and n. The spectrum of the MHD waves trapped in the Sun may be maintained by the combined effect of this energy cascade and the loss of energy in the form of the emerging flux tubes. The primary energy input into the spectrum may be occurring in the mode $\{l = 1, 3, 5, 7; n = 1)$. As expected from the above phenomenological model, the size of a sunspot cycle and its excess over the previous cycle are well correlated (e.g., $\sim 90\%$) to the phase-changes of the two most dominant oscillation modes during the previous one or two cycles. These correlations may provide a physical basis to forecast the cycle sizes.

1. Introduction

From the Legendre–Fourier (LF) analysis of the magnetic field ('$B_{\rm inf}$') inferred from sunspot data during 1874–1976 it has been shown earlier (Gokhale *et al.*, 1992, Paper I) that the sunspot activity may be originating in the interference of Sun's global magnetic oscillations represented by sets of LF terms in $B_{\rm inf}$ having odd degrees ('l') and frequencies close to ν_* ($\approx 1/21.4$ y) and to a few odd harmonics of ν_*. In Paper II (Gokhale and Javaraiah, 1992) it was shown that the superposition of the dominant LF terms of frequency ν_*, with average amplitudes and phases during 1874–1976, can reproduce not only the average butterfly diagram but also the observed average behavior of the magnetic field in *middle* and *high* latitudes (e.g., the poleward migrations of the weak fields, the polar activity cycle and the polar reversals, all in the right phases) even though the data used for determining the LF terms in the 'inferred' magnetic field is only from

Solar Physics **156:** 157–177, 1995.

the low ($< 35°$) latitudes. This indicated that the computed LF terms in B_{inf} may be representing a set of real global MHD oscillations of the Sun and not merely a mathematical transform of the latitude-time distribution of the data.

In the present paper we examine the following questions which would arise if the solar magnetic cycle is really a consequence of superposition of global MHD oscillations.

(i) How would superposition of global MHD oscillations lead to formation and emergence of the magnetic flux tubes that produce the solar activity ? What kind of MHD oscillations are needed for this purpose ?

(ii) How is the rate of production of activity related to the amplitudes and phases of the superposed oscillations (waves)?

(iii) What set of LF terms represents the set of the global waves that produces most of the observed sunspot activity?

(iv) What minimal set of LF terms can be used to model the variation of the amount of the annual sunspot activity during each sunspot cycle (i.e., the '*shapes*' of the sunspot cycles)?

(v) How is the spectrum of the global waves maintained?

(vi) Which LF terms represent the primarily excited waves?

(vii) Can the analysis be used for forecasting the amount of sunspot activity?

In this investigation a key step is to model the observed variations in the rate of production of sunspot activity ('shapes' and 'sizes' of the sunspot cycles). For this it is necessary to modify the normalization of the 'inferred magnetic field' (B_{inf}) as explained in Section 2.1. The 'renormalized B_{inf}' which we denote as '$Q(\theta, t)$' represents 'the rate of toroidal flux emergence above the photosphere': i.e., the amount of toroidal magnetic flux emerging above the photosphere per unit latitude interval, per unit time.

In Section 2.2 we describe how the interference of a set of the Sun's global MHD oscillations (e.g., torsional MHD oscillations) can result in intermittent emergence of toroidal magnetic flux in the form of flux tubes. We also show how the rate of flux emergence $Q(\theta, t)$, on sufficiently large scales of length and time, will be related to the amplitudes and phases of the global oscillations (represented by Legendre–Fourier terms in the toroidal field component B_Φ) and how the latter amplitudes and phases can be studied using the LF terms in 'Q' computed from the sunspot data.

In Section 2.3 we develop a method to model the 'shapes' of the sunspot cycles by superposing any prescribed set of LF terms in $Q(\theta, t)$, using the amplitudes and phases during each cycle as computed from the sunspot data.

In Section 2.4 we use Parceval's theorem to identify $\{l = 1, 3, \ldots, 13; n = 1, 3, 5\}$ as the set of terms in B_Φ that represents the waves which, through the process suggested in Section 2.2.1, could contribute most of the observed sunspot activity.

In Section 2.5 we show that for modeling satisfactorily the observed 'shape' of any of the nine cycles with amplitudes and phases of a minimum number of LF

terms, the terms with $l = 3$ (or 3, 5) and $n = 1$, 3 (or 1, 3, 5) are necessary and sufficient.

The above minimization of terms is possible due to coherence in the variations of the amplitudes and phases of the terms *within* each of the following four groups (Section 3.1):

$$\{l = 1, 3, 5, 7;\ n = 1\}, \qquad \{l = 1, 3, 5, 7;\ n = 3\},$$

$$\{l = 9, 11, 13, 15;\ n = 1\}, \quad \{l = 9, 11, 13, 15;\ n = 3\},$$

and correlations of the amplitudes and phases of terms in each group with those of the terms in the other groups.

Using the phase coherence, we show in Section 3.2, that these groups represent four modes of global oscillations.

In Section 4.1 we point out the possibility of the existence of a cascade of energy in the LF spectrum. The mutual correlations among the amplitudes and phases of the above four oscillation modes suggest the existence of such a cascade (Section 4.2).

In Section 4.3 we point out how the emergence of flux tubes by the process described in Section 2.2.1 will yield *surface fields* and *solar activity*, as well as removal of energy from the interfering waves causing *shifts* in their phases.

In Section 4.4.1 we suggest a phenomenological model for maintenance of the LF spectrum by the cascade and the removal of energy assuming a supply of energy through some fundamentally excited waves of lower l and ν. In Section 4.4.2 we identify $l = 3, 5; n = 1$) as the dominant terms among the fundamentally excited waves.

If the LF spectrum is really maintained as suggested here, then there should be correlations between the size of a sunspot cycle and the changes in the phases of the LF terms during the previous one or two cycles (Section 4.5.1). In Sections 4.5.2 and 4.5.3 we show that such correlations indeed exist. In fact, these correlations might even be useful for forecasting the size of a sunspot cycle on a physical basis (Section 4.5.4).

In Section 5 we summarize the proposed phenomenological model and discuss its implications and limitations. Reasons are given why the global MHD waves described here by the LF terms may be real, and 'torsional'. A conjecture about the mechanism of excitation of the low l, n modes is also given for the sake of completeness of the proposed model.

2. Modeling the Variation of the Annual Measure of Sunspot Activity

2.1. The 'flux emergence rate' $Q(\theta, t)$, inferred from data, and its Legendre–Fourier analysis

In Papers I and II the sunspot occurrence probability during any given time interval was normalized to the total amount of activity in that time interval. Thus the unit of B_{inf} varied from cycle to cycle, depending upon the 'size' of the cycle. This was fine for studying the latitude-time distribution of activity during any single time interval irrespective of the total amount of activity during that interval. However, for modeling the *variations* in the *rate of production* of sunspot activity) the total probability in any given time interval should be proportional to the total measure of activity in that time interval. Hence, we renormalize the sunspot occurrence probability in the following manner.

Consider length scales *large* compared to the dimensions of the spot groups and time scales large compared to the lifetimes of the spot groups but *small* compared to the durations of the sunspot cycles (e.g., length scales $\geq 10^4$ km and time scales $\geq$ a few months). On such scales we define the sunspot occurrence probability, as a function of latitude and time, as follows:

$$\begin{aligned} \mathcal{P}(\theta, t) &= \tau_k \delta(\theta - \theta_k, t - t_k) && \text{in the neigborhood of } (\theta_k, t_k)\ , \\ &= 0\ , && \text{elsewhere}\ , \end{aligned}$$

where θ_k, t_k are the values of θ and 't' for the spot group 'k', τ_k is the life span of the spot group 'k', and δ represents the Dirac delta function. As required, the integral of $\mathcal{P}(\theta, t)$ over the unit sphere during any time interval is proportional to the measure of sunspot activity during that interval.

This probability function is related to the sunspot occurrence probability function $p(\theta, t)$ of Paper I in the following way:

$$\mathcal{P}(\theta, t) = (\Sigma_k \tau_k) p(\theta, t)\ ,$$

where the summation Σ_k extends over *all* the spot groups observed *during* a given time interval, or during a given sunspot cycle.

We take τ_k as a reasonable measure of the amount of magnetic flux which emerges above the photosphere (and leaves the Sun), in association with the appearance and disappearance of the spot group 'k'. From the generally bipolar nature of the fields associated with activity, it is believed that the emerging flux is toroidal.

In analogy to $B_{\text{inf}}(\theta, t)$ in Papers I and II, we then define a quantity $Q(\theta, t)$ as

$$Q(\theta, t) = \pm \mathcal{P}(\theta, t)\ , \tag{1}$$

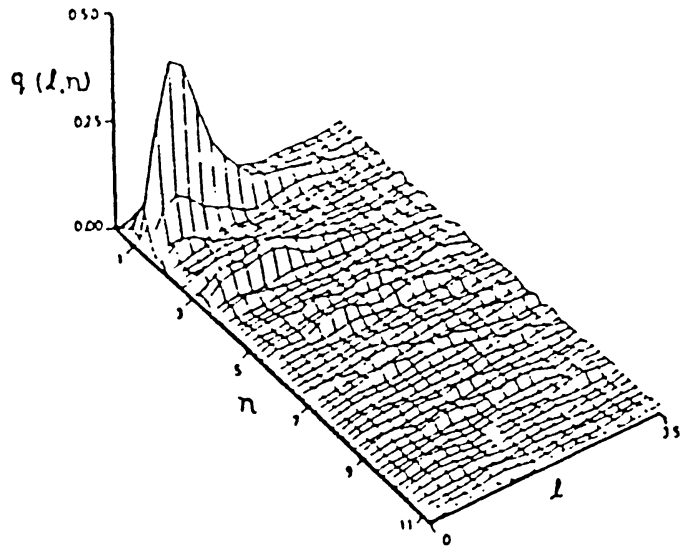

Fig. 1. The average Legendre–Fourier spectrum of the relative amplitudes $q(l, n)$ of $Q(\theta, t)$ during 1874–1976. This spectrum is the same as that of the relative amplitudes of $B_{\text{inf}}(\theta, t)$ given in Paper I.

where the signs $\pm$ are chosen according to Hale's laws of magnetic polarities. Clearly, on time scales $\geq$ a few months and length scales $\geq 10^4$ km, $Q(\theta, t)$ represents a measure of '*the amount of the toroidal magnetic flux emerging above the photosphere at* (θ, t), per unit latitude interval per unit time'. Equation (1) can also be written as

$$Q(\theta, t) = (\Sigma_k \tau_k) B_{\text{inf}}(\theta, t) \, .$$

2.1.1. *Amplitudes and Phases of Legendre–Fourier Terms during Each Sunspot Cycle*

Using the method given in Papers I and II we have determined the amplitudes $q(l, n)$ and the phases $\phi(l, n)$ of the axisymmetric SHF terms (i.e., LF terms) of odd degrees, $l = 1$ to 29, and frequencies $\nu = n\nu_*$ $(n = 1, 3, 5, 7)$ in $Q(\theta, t)$, *during each of the nine sunspot cycles* between 1879 and 1976. During each cycle, the spectrum of the *relative amplitudes* in 'Q' is similar to (but not the same as) that during the whole sequence of the 103 years. Owing to the above relation between Q and B_{inf}, the latter spectrum is the same as the *relative amplitude* spectrum of B_{inf} during the 103 years which was shown in Figure 1 of 'Paper I', and which is reproduced here for convenience (Figure 1).

2.2. A MODEL OF TOROIDAL FLUX EMERGENCE AS PROVIDED BY INTERFERENCE OF TORSIONAL MHD OSCILLATIONS

2.2.1. *Formation of Toroidal Flux Tubes and Their Emergence*

Consider a set of axi-symmetric MHD oscillations (e.g., torsional), each represented, during each cycle, by a set of LF terms, and described *collectively* by the sets

$\{l\}$ and $\{n\}$ of the values of l and n, respectively. The toroidal magnetic field B_Φ at a point (r, θ), at an instant 't' during a cycle 'i', can be written as

$$B_\Phi(i;\, r,\, \theta,\, t) = \Sigma_{\{l\}}\Sigma_{\{n\}} b(i;\, l,\, n) f_{l,n}(r) \times \\ \times P_l(\mu) \sin[2\pi n \nu_* t + \epsilon(i;\, l,\, n)] \,, \tag{2}$$

where $b(i;\, l,\, n)$ and $\epsilon(i;\, l,\, n)$ represent the amplitudes and the '*initial*' phases of the terms $(l,\, n)$ in 'B_{inf}', during the cycle 'i'; $f_{l,n}(r)$ is the radial eigenfunction for the mode $(l,\, n)$ and $\mu = \cos\theta$.

At θ and 't' where the interference creates a toroidal flux bundle whose magnetic buoyancy overcomes its magnetic tension, the flux bundle will emerge above the photosphere.

2.2.2. *The Rate of Emergence of Toroidal Flux*

Let τ_{max} be the maximum time required for any such toroidal flux bundle, after its creation, to emerge above the photosphere at all longitudes. Since the large-scale meridional flows in the Sun's radiative core are negligible, the amount of toroidal flux across any meridional section of the radiative core must remain constant. Hence, on time scales $> \tau_{\text{max}}$, and less than the diffusion time scales, the amount of the toroidal flux $Q(\theta,\, t)\mathrm{d}\theta$, emerging above the photosphere per unit time across a latitude interval $\mathrm{d}\theta$, will be given by

$$Q(\theta,\, t)\, \mathrm{d}\theta = \partial \left[\int_0^R B_\Phi(r,\, \theta,\, t) r \, \mathrm{d}\theta \, \mathrm{d}r \right] \Big/ \partial t \,,$$

where $r = R$ is the radius of the base of the convective envelope. Hence, for modeling the sunspot cycles, the flux emergence rate $Q_{\text{mod}}(i;\, \theta,\, t)$ during any cycle 'i' can be written, using Equation (2), as

$$Q_{\text{mod}}(i;\, \theta,\, t) = \Sigma_{\{l\}}\Sigma_{\{n\}} b(i;\, l,\, n) g_{l,n}(R) \times \\ \times 2\pi n \nu_* P_l(\mu) \cos[2\pi n \nu_* t + \epsilon(i;\, l,\, n)] \,, \tag{3}$$

where

$$g_{l,n}(R) = \int_0^R f_{l,n}(r) r \, \mathrm{d}r \,.$$

2.2.3. *Relations between the LF Terms in 'Q' and Those in 'B_Φ'*

Equation (3) can be rewritten as

$$Q_{\text{mod}}(i;\, \theta,\, t) = \Sigma_{\{l\}}\Sigma_{\{n\}} q(i;\, l,\, n) \times \\ \times P_l(\mu) \sin[2\pi n \nu_* t + \phi(i;\, l,\, n)] \,,$$

where

$$q(i;\, l,\, n) = 2\pi n \nu_* b(i;\, l,\, n) g_{l,n}(R) \tag{4a}$$

and

$$\phi(i;\, l,\, n) = \epsilon(i;\, l,\, n) + \pi/2\,. \tag{4b}$$

It follows that according to this model, (i) the sets of terms $\{l\}$ and $\{n\}$ of appreciable amplitudes in the LF spectrum of B_Φ will be same as those obtained through the LF analysis of 'Q', but (ii) owing to the factor $g_{ln}(R)$ in (4a), the ratios of amplitudes ('b's) of different LF terms in 'B_Φ' may not be same as those of the amplitudes ('q's) of the corresponding terms in 'Q', and (iii) the temporal variations and relative differences in the phases of LF terms in B_Φ will be same as those in the phases of the corresponding terms in $Q(\theta,\, t)$.

2.2.4. *The Torsional MHD Nature of the Oscillations*

The only observed large-scale flows that can, in principle, create toroidal fields are the 'torsional waves' of '11-yr' periodicity (LaBonte and Howard, 1982), or '22-yr' periodicity (Javaraiah and Gokhale, 1994) detected in the photospheric rotation. Rotational perturbations on time scales of years seem to exist even in the solar interior (Dziembowskii and Goode, 1992). In the presence of even a very weak but sufficiently long-lived poloidal field with $l = 1$ and 3 (e.g., Mestel and Weiss, 1987; Spruit, 1990; Gokhale and Hiremath, 1992; Hiremath and Gokhale, 1995), such perturbations would constitute torsional MHD waves.

Thus, if the LF terms in 'B_Φ' represent global oscillations/waves, then these must be 'torsional' MHD in nature.

2.3. Method to Model the 'Shapes' and 'Sizes' of the Individual Sunspot Cycles by Recombining any Prescribed Set $\{l,\, n\}$ of LF Terms in 'Q'

It follows from Equation (1) that the sunspot occurrence probability *per latitude interval of unit photospheric area per unit time*, at colatitude 'θ', at time 't', will be given by

$$\mathcal{P}_{\text{mod}}(\theta,\, t) = |Q_{\text{mod}}(\theta,\, t)|\,. \tag{5}$$

Hence in a model combining a prescribed set $\{l,\, n\}$ of LF terms the sunspot

occurrence probability, p_{mod}, at the central epoch 't_{ijk}' of the kth 'month' in the jth year of the ith cycle can be written as

$$p_{\text{mod}}(\{l\}, \{n\}; i, j, k) = T \int_{45°}^{135°} |Q_{\text{mod}}(i; \theta, t_{ijk})| \sin\theta \, \mathrm{d}\theta =$$

$$= 2T \int_{45°}^{90°} |\Sigma_{\{l\}}\Sigma_{\{n\}} q(i; l, n) P_l(\mu) \sin[2\pi n \nu_* t_{ijk} + \phi(i; j, k)]| \sin\theta \, \mathrm{d}\theta \, . \quad (6)$$

Here the term 'month' means any given 1/12 part of a year and 'T' is its length.

The limits of integration with respect to the colatitude are chosen so as to exclude the low-level flux concentrations outside the sunspot zone which are not strong enough to be seen as sunspot activity (see Paper II), and the symmetry of the integrand is used for changing the limits of the integral.

The annual measure of the sunspot occurrence probability is

$$s_{\text{mod}}(\{l\}, \{n\}, i, j) = \sum_{k=1}^{12} (\{l\}, \{n\}, i, j, k) \, . \quad (7)$$

The variation of $s_{\text{mod}}(\{l\}, \{n\}; i, j)$ with 'j' gives the 'reconstructed shape' of the sunspot cycle 'i' for a given choice of $\{l\}$ and $\{n\}$.

The 'size' of the cycle 'i' in the reconstructed model will then be given by

$$S_{\text{mod}}(\{l\}, \{n\}, i) = \sum_j s_{\text{mod}}(\{l\}, \{n\}; i, j) \, . \quad (8)$$

2.4. Identification of the set of significant LF terms in 'Q' that account for most of the observed sunspot activity

According to Parceval's theorem, the size $S_{\text{mod}}(i)$ of a sunspot cycle 'i' in the recombination model must be proportional to the total LF power in the set $[\{l\}, \{n\}]$ of terms taken in Equation (6). Thus

$$P(i; \{l, n\}) = \sum_{\{l\}, \{n\}} [q(i; l, n)]^2 \, .$$

Starting from a set of lowest l and n, the correlation between $P(i; \{l, n\})$ and the observed size of the cycle i, viz., $S_{\text{obs}}(i)$, first increases with inclusion of terms with higher and higher l and n. A stage comes when the correlation starts dropping down due to larger relative errors in the amplitudes of the higher terms. From the

maximum correlation we have identified $\{l = 1, 3, \ldots, 13; n = 1, 3, 5\}$ as the set of LF terms in 'Q' which are significant in modeling by recombination of LF terms. The high ($\sim 99.98\%$) correlation assures that the significant set is adequate to account for most of the observed sunspot activity.

2.5. Comparison between the modeled and the observed 'shapes'

For each cycle 'i' we have modeled the 'shape' $s_{\text{mod}}(i, j)$ and the 'size' $S_{\text{mod}}(i)$ with various choices of $\{l\}$ in the range 1 to 13 and $\{n\}$ in the range 1, 3, 5.

For determining the 'observed shape' of a cycle 'i' we take the sum $s_{\text{obs}}(i, j)$ of the life-spans (in days) of all the spot groups born during the jth year of the cycle 'i' as the measure of the sunspot activity during that year.

For each of several choices of the sets $\{l\}$ and $\{n\}$, we have computed the coefficients of correlation between $s_{\text{mod}}(\{l\}, \{n\}; i, j)$ and $s_{\text{obs}}(i, j)$ during each cycle 'i'. We have also computed the correlation between $S_{\text{mod}}(\{l\}, \{n\}, i)$ and $S_{\text{obs}}(i)$ for $i = 1$ to 9. The results are given in the next two subsections.

2.5.1. *Importance of the Terms with* $n = 1, 3, 5$

We have found that during each cycle 'i' the correlation between the modeled 'shape' $s_{\text{mod}}(\{l\}, \{n\}; i, j)$ and the observed 'shape' $s_{\text{obs}}(i, j)$, for $j = 1$ to 11, is $> 80\%$ for any choice of $\{l\}$ in the range $l = 1$ to 13 with $n = 1$. As expected from the asymmetries of the sunspot cycles (Bracewell, 1988), inclusion of corresponding terms with $n = 3$ increases the correlations substantially (e.g., by $> 4\%$) whereas improvements by further inclusion of $n = 5$ are only marginal (e.g., $< 1\%$). Still further improvement by inclusion of higher terms ($n > 7$), will be negligible since their amplitudes are quite small. Thus, terms of $l = 1, \ldots, 13$ and $n = 1, 3$ (or $n = 1, 3, 5$), are adequate for modeling the shapes of the cycles.

2.5.2. *The Optimal Set* $\{l, n\}$ *That Gives the Best Correlation*

Among the nearly highest correlations given by the different choices of $\{l, n\}$ with l in the range $l = 1, \ldots, 13$, and $n = 1, 3$, the subset $\{l = 3; n = 1, 3\}$ or $\{l = 3, 5; n = 1, 3\}$ gives the highest correlation (~ 0.97) between s_{mod} and s_{obs} during each of the nine cycles. The latter subset gives the highest average correlation between the observed and the modeled shapes over the whole sequence of the nine cycles (see Figure 2). However, the differences between the correlations given by the two subsets seem too small to be significant (see Table I).

Hence, during every cycle the shape consisting of the eleven observed points (*ten relative values*) can be equally well reproduced by specifying *only four parameters*, viz., the amplitudes and phases of $\{l = 3; n = 1, 3\}$.

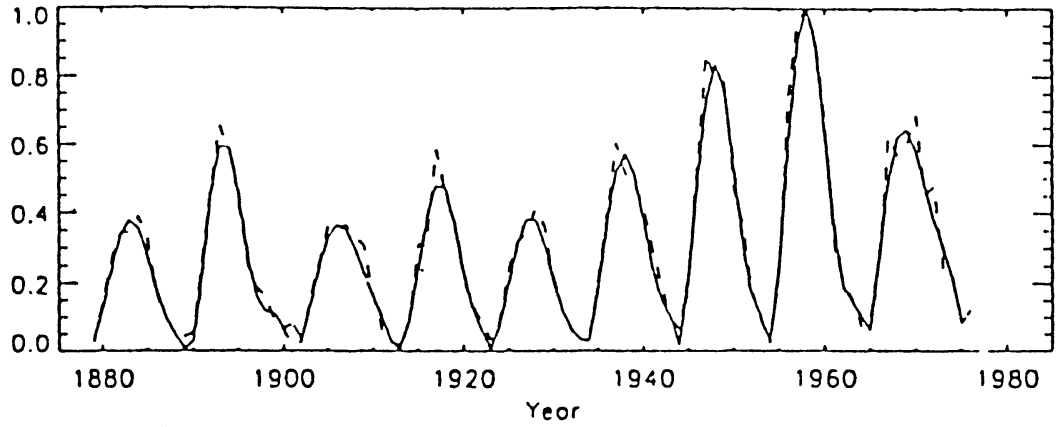

Fig. 2. Variation of $s_{obs}(i, j)$ (dashed line), and that of $s_{mod}(i, j)$ (continuous line), both normalized to their values in 1958, during sunspot cycles $i = 12$ to 20. For each cycle the model uses amplitudes and phases of only $\{l = 3, 5; n = 1, 3\}$. Agreement from the model using $\{l = 3; n = 1, 3\}$ only will be almost equally good (see Section 2.5.2).

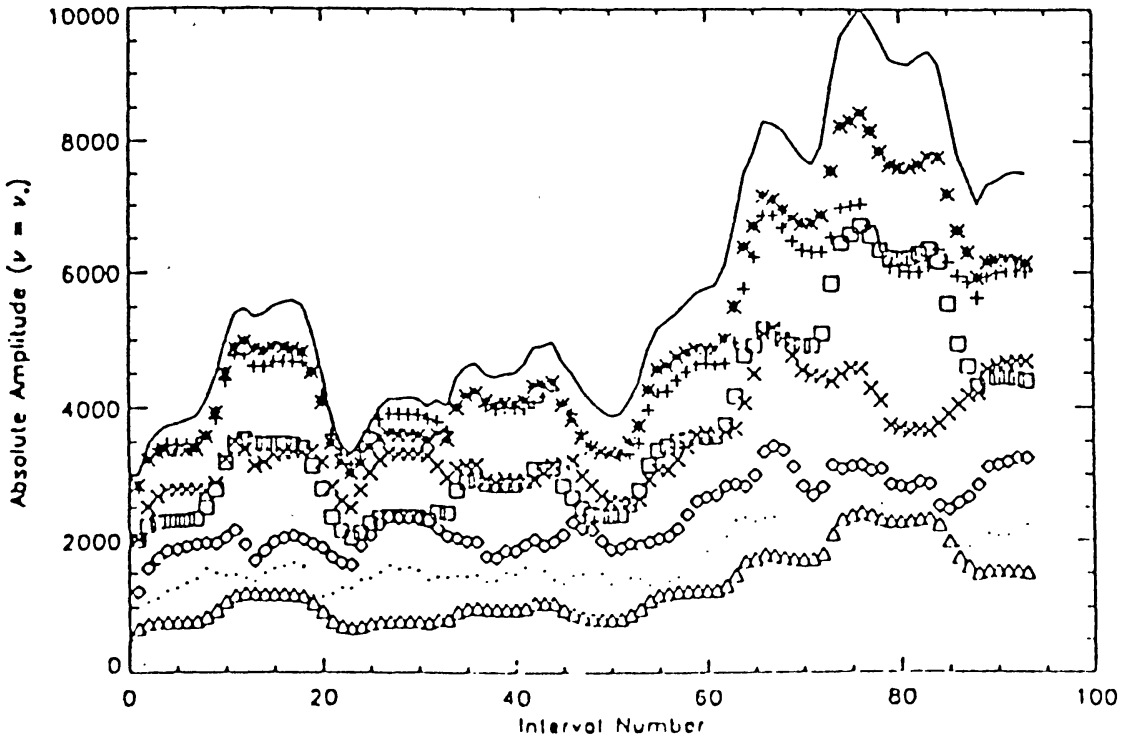

Fig. 3. Temporal variation of the amplitudes $q(l, n)$, for $n = 1$, as represented by values during 11-yr intervals successively displaced by 1 yr. The symbols △, □, ∗, +, ×, diamond, and dot, represent $l = 1, 3, 5, 7, 9, 11$, and 13, respectively. The continuous curve represents the values of the amount of observed sunspot activity (S_{obs}) during the respective intervals.

3. The Stationary Oscillations

3.1. High mutual correlations between the amplitudes and phases of terms with different l but same n

The high correlations between the modeled and the observed shapes for any subset of $\{l\} = \{1, 3, \ldots, 13\}$ noted in Section 2.5 suggest the presence of high mutual

TABLE I

The coefficients of correlations between the observed 'shapes' of the cycles (Waldmeier numbers) $i = 12, 13, \ldots, 20$, and those reconstructed using sets $\{l = 3, n = 1, 3\}$ and $\{l = 3, 5; n = 1, 3\}$

Cycle No.	$\{l = 3; n = 1, 3\}$	$\{l = 3, 5; n = 1, 3\}$
12 (1879–1889)	0.973	0.980
13 (1890–1901)	0.984	0.983
14 (1902–1912)	0.968	0.976
15 (1913–1922)	0.959	0.959
16 (1923–1933)	0.968	0.981
17 (1934–1943)	0.966	0.973
18 (1944–1953)	0.983	0.979
19 (1954–1964)	0.993	0.991
20 (1965–1976)	0.939	0.954
Average	0.970	0.975

correlations among the amplitudes and phases of the LF terms in this range of l for each n.

Such high mutual correlations are indeed seen in Figures 3 and 4 showing, for $n = 1$, the variations in the amplitudes $q(l, n)$ and phases $\phi(l, n)$ determined from 11-yr intervals successively displaced by 1 yr.

Mutual correlations are also seen in the similarly determined variations of the phases $\phi(l, n)$ of the terms of different l for $n = 3$ shown in Figures 5(a) and ((b).

3.2. Existence of Resonant and Approximately Stationary Global Oscillations in B_Φ

In view of Equation (4b), the phase variations in Figures 4 and 5 can be considered also as the variations in the *initial* phases $\epsilon(l, n)$ of LF terms in B_Φ.

Further, we see in Figures 4 and 5 that the terms $l = 1, 3, \ldots, 15$, $n = 1, 3$ form four separate groups ($l = 1, 3, 5, 7$; $n = 1$), ($l = 9, 11, 13, 15$; $n = 1$), ($l = 1, 3, 5, 7$; $n = 3$) and ($l = 9, 11, 13, 15$; $n = 3$), such that terms within each group have mutual 'phase coherence', with successive phase differences of $\approx \pm 180°$, and a certain common degree of 'phase constancy'.

Hence, the expression on the right-hand side of Equation (2) can be written, collecting the terms in each group, as

$$B_\Phi(i;\, r,\, \theta,\, t) = B_{\mathrm{I},\,1}(r,\, \mu)\sin(2\pi\nu_* t + \lambda_{1,\,1}) + B_{\mathrm{II},\,1}(r,\, \mu)\sin(2\pi\nu_* t + \\ + \lambda_{2,\,1}) + B_{\mathrm{I},\,3}(r,\, \mu)\sin(2\pi 3\nu_* t + \lambda_{1,\,3}) + \\ + B_{\mathrm{II},\,3}(r,\, \mu)\sin(2\pi 3\nu_* t + \lambda_{2,\,3}) + \cdots\,,$$

where

$$B_{\mathrm{I},\,1}(r,\, \mu) \equiv \{b_{1,\,1} f_{1,\,1}(r) P_1(\mu) - b_{3,\,1} f_{3,\,1}(r) P_3(\mu) + \\ + b_{5,\,1} f_{5,\,1}(r) P_5(\mu) - b_{7,\,1} f_{7,\,1}(r) P_7(\mu)\}\,,$$

$$B_{\mathrm{II},\,1}(r,\, \mu) \equiv \{b_{9,\,1} f_{9,\,1}(r) P_9(\mu) - b_{11,\,1} f_{11,\,1}(r) P_{11}(\mu) + \\ + b_{13,\,1} f_{13,\,1}(r) P_{13}(\mu) - b_{15,\,1} f_{15,\,1}(r) P_{15}(\mu)\}\,,$$

and similar expressions for $B_{\mathrm{I},\,3}(r,\, \mu)$ and $B_{\mathrm{II},\,3}(r,\, \mu)$ from the other two groups. Here b_{ln} and λ_{ln} are the mean values of the amplitudes $b(i;\, l,\, n)$ and phases $\epsilon(i;\, l,\, n)$, respectively, defined in Equations (4a) and (4b), all of which must be approximately constant in time, since $q(i;\, l,\, n)$ and $\phi(i;\, l,\, n)$ are so. Clearly, each of the four terms on the right-hand side represents a stationary global oscillation in 'B_Φ'.

4. Phenomenological Model for Maintenance of the LF Spectrum and Production of Activity

4.1. Possibility of Existence of Cascade of Energy in the LF Spectrum

In the Sun, the density falls off rapidly near the photosphere. The intensity of the background field may not vary much (e.g., Gokhale and Hiremath, 1993). Hence, if torsional MHD waves are excited inside the Sun, their phase speed would increase rapidly as they approach the photosphere. Hence the waves will be trapped inside the sun by total internal reflections at the photosphere. In general the angles of incidence will be non-zero, and hence the reflected waves will have different values of l than the incident waves. This transfer of energy will continue during successive reflections provided there is a continued supply of energy at the original 'l'. In the whole process, appreciable energy will be stored only in the normal modes of global oscillations (for which higher l corresponds to higher ν). Since the dissipation occurs at high l and ν, the overall transfer of energy will constitute a cascade from modes of lower l, ν to those of higher l, ν.

4.2. Evidence for Existence of Cascade of Energy in the LF Spectrum

There are high correlations among the phases (and also among the amplitudes) of LF terms of low and high values of l (Section 3.1) and among the terms of low and high values of n (Gokhale and Javaraiah, 1990).

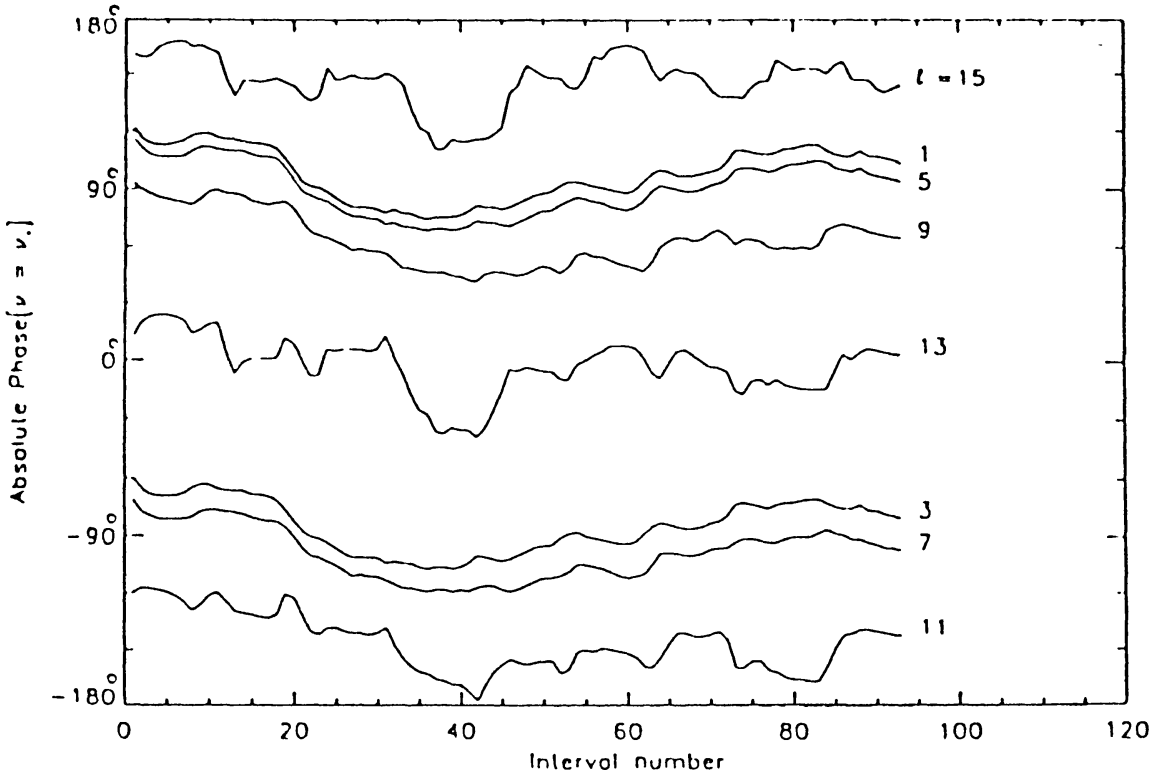

Fig. 4. Temporal variation of the phases $\phi(l, n)$, or $\epsilon(l, n)$ of the terms $l = 1, 3, \ldots, 15$, all with $n = 1$, during the 11-yr intervals successively displaced by 1 yr.

If we examine Figure 4 carefully, we find *increments* and *decrements* of the *initial phases* of terms in $n = 1$ occurring during intervals of lengths $\sim$ 7 yr and $\sim$ 4–5 yr. These variations imply *decelerations and accelerations*, respectively, in the phase speeds of the waves of the frequency ν_* on time scales *corresponding to* $3\nu_*$ and $5\nu_*$. Accelerations and decelerations in the phase speeds of the terms in $\nu = 3\nu_*$ in Figure 5 are also seen to occur during exactly the same intervals of time. Thus the correlations which exist for each l in the phase variations of the lower and the higher n (e.g., $\sim$ 85–90% between $n = 1$ and 3; Gokhale and Javaraiah, 1990), seem to be due to the simultaneous phase accelerations and phase decelerations of the waves of the lower and the higher n. Thus the phase variations in Figures 4 and 5 indicate transfer of energy from LF terms of $3\nu_*$ and $5\nu_*$.

Similarly the mutual correlations between the amplitudes and phases of LF terms of different l, and same n, imply transfer of energy from waves of lower 'l' to those of higher l, with the same ν.

4.3. Production of Surface Fields and Activity, Creation of Phase Shifts due to Emergence of Flux Tubes

4.3.1. *Production of Surface Fields and Activity*

Whenever the flux bundles formed by interference of MHD waves emerge above the photosphere by the process envisaged in Section 2.2.1, they will be seen as

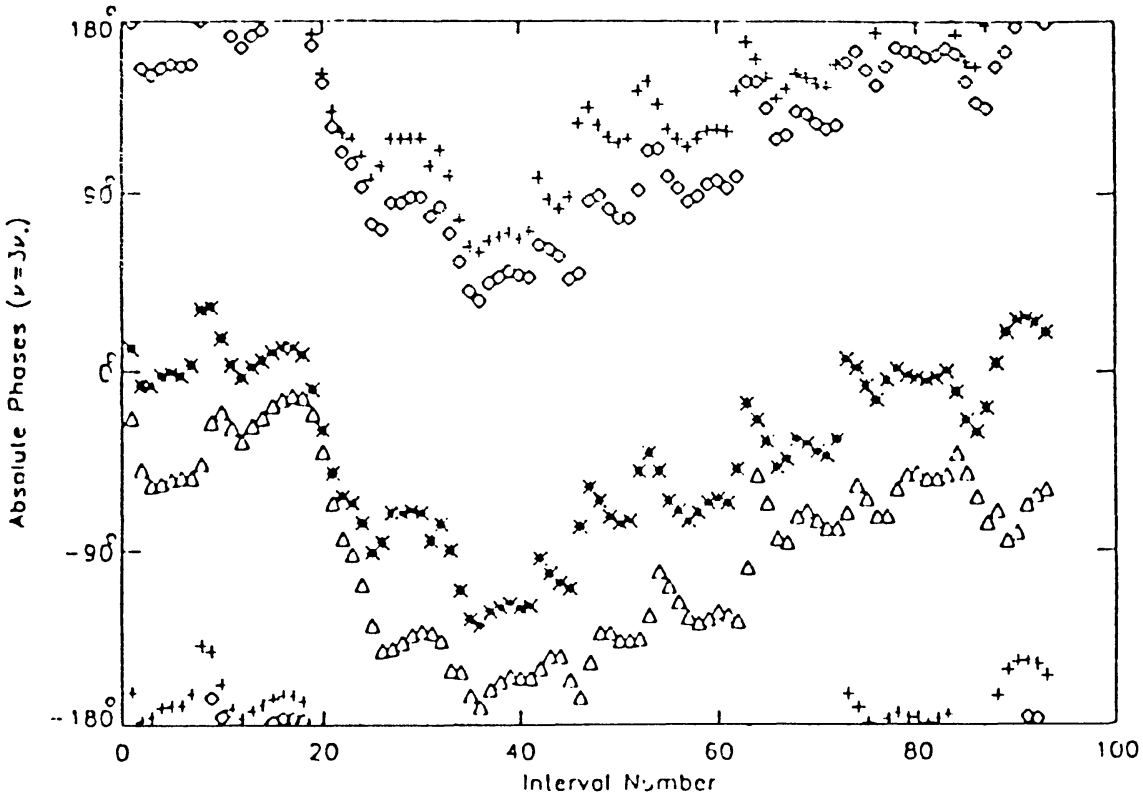

Fig. 5a.

Fig. 5a–b. Temporal variation of the phases $\phi(l, n)$, or $\epsilon(l, n)$, of the third harmonic ($n = 3$) terms as represented by values during 11-yr intervals successively displaced by 1 yr. In (a), symbols +, *, diamond, and △ represent $l = 1$, 3, 5, and 7, respectively. In (b) they represent $l = 9$, 11, 13, and 15, respectively.

'surface fields'. The dissipation of the emerged flux bundles in the atmosphere will produce 'activity' of various types on various scales.

4.3.2. *Production of 'Photospheric Fields' and 'Activity' That Are Regularly Distributed in Latitudes and Time*

The 'toroidal flux bundles' given by interference of the waves with non-random phase variations will be regularly distributed in latitude and time. Thus the modes with $\nu = \nu_*$, $3\nu_*$, and $5\nu_*$, would yield the observed 'photospheric fields' and 'activity' that are distributed regularly in latitudes and in time, viz., (i) sunspot activity distributed in 'butterfly diagrams', (ii) 'weak' fields appearing to migrate towards the poles, and (iii) the 'reversing' polar fields. (This is already shown, up to the terms in ν_* alone, for $l = 1$ to 13 by Stenflo (1988), and for $l = 1$ to 29 by us in Paper II.)

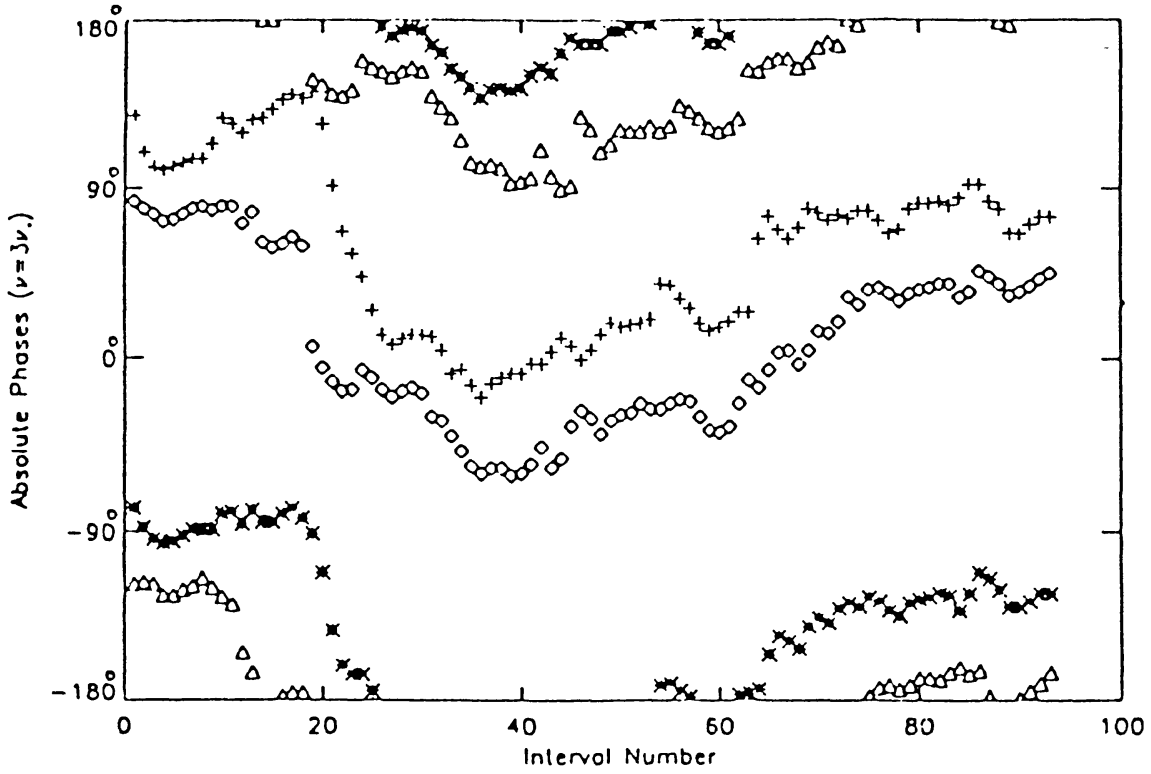

Fig. 5b.

4.3.3. *Production of Randomly Distributed Small-Scale Photospheric Fields and Activity*

Since the waves with $n > 5$ have random phases (Section 4.3.5), the flux tubes formed by their interference may be producing the small-scale fields and activity distributed randomly on the surface, and in time (may be, e.g., 'bright points' in X-ray and EUV emissions).

4.3.4. *Removal of Energy from Interfering Waves and Creation of Phase-Shifts*

The emergence of flux tubes as in Section 2.2.1 implies sudden removal of energy, viz., the magnetic energy of the flux tubes, from the interfering waves. Since this occurs on time scales ($\tau_{\max}$: Section 2.2.2) much shorter than the wave periods, this would lead to 'changes' in the phases of the respective terms in the LF spectrum.

4.3.5. *The Observed Phase Changes*

We have determined the cycle-to-cycle 'shifts' in the phases, ϵ_{ln}, from changes in ϕ_{ln}, using Equation 4(b). These are $< 30°$ for $n = 1$, $\approx 30°$–$90°$ for $n = 3$, and $90°$–$120°$ for $n = 5$. For $n > 5$ the phase changes are $> 120°$ and, hence, essentially random.

For each LF term, the observed cycle-to-cycle phase change will be the net result of the energy received from terms of lower l, n, energy contributed to the emerging flux tubes, and energy passed on to the terms of higher l, n.

4.4. MAINTENANCE OF THE LF SPECTRUM AND THE DOMINANT TERMS IN THE BASICALLY-EXCITED OSCILLATION

4.4.1. *Maintenance of the LF Spectrum*

The foregoing discussion suggests that the LF spectrum of the global oscillations is a net result of (i) input of energy at some low l, ν, (ii) cascade of energy from lower l, ν to higher and higher l, ν, and (iii) intermittent removal of energy from the waves in the form of toroidal flux tubes formed by interference.

4.4.2. *The Dominant LF Terms in the Basically Excited Oscillation and the Approximate Balance between Inputs and Outputs of Energy*

In Figure 2 we also see that the amplitudes $q(l, n)$ for $n = 1$ and $l = 1$–13 determined from 11-yr long time intervals succcessively displaced by 1 yr show high correlations with the measure of sunspot activity, S, during those intervals. Actually, these correlations are expected from the definition of $q(l, n)$. However, among these, the best correlation is given by amplitudes of $l = 3$ and 5 and not by the largest two amplitudes in 'Q', viz., of $l = 5$ and 7 (see Figure 1). Thus the energy in $\{l = 3, 5; n = 1\}$ seems to control the variation of the amount of sunspot activity even on time scales $\geq$ 11yr. This, along with the result of Section 2.5.2, shows that $\{l = 3, 5; n = 1\}$ may be the dominant terms in the basically excited waves.

The same correlation also suggests that on time scales $>$ 11 yr there may be a fairly good balance between the rate of energy input into ($l = 3, 5$; $n = 1$) and that of energy disposal through sunspot activity. [Evidence for the Associated 'Torsion': It may be noted that the terms $\{l = 3, 5; n = 1\}$ belong to the mode $\{l = 1, 3, 5, 7; n = 1\}$ in B_Φ which corresponds to $\{l = 2, 4, 6; n = 1\}$ in the rotational angular velocity (i.e., the 'torsional oscillation' of '22-yr periodicity'). In the analysis of surface rotation the presence of such an oscillation is indicated by that of 22-yr periodicity in the coefficient of $\sin^2\theta$ (Javaraiah and Gokhale. 1994).]

4.5. TESTS OF THE PHENOMENOLOGICAL MODEL AND THEIR VERIFICATION

4.5.1. *Correlations Expected between the 'Cycle Size' and the 'Phase-Changes'*

Since the changes in the phases of LF terms with $n = 1$ and 3 are not large (see Section 4.3.5), these phase changes can serve as measures of the net effect of the gains and losses of energy by these terms. Hence, according to the foregoing model of energy cascade and production of activity (Sections 4.2 and 4.3), the following correlations should exist.

Test 1: the size of a sunspot cycle should be proportional to the amount of energy lost by *all* those waves whose interference creates the sunspot activity during that cycle. Hence $S_{\rm obs}(i)$ should be correlated to the phase changes of the corresponding LF terms from cycle '$i - 1$' to cycle 'i'.

Test 2: also, the change in the cycle size from one cycle to the next cycle should be correlated to the phase shifts of the terms representing those waves of $n = 1$ into which the energy is input during some earlier cycles.

4.5.2. *Verification of the 'Test 1'*

For verifying *Test 1* we have determined the coefficients of correlations of $S_{\text{obs}}(i)$ with the sums of the changes $\Delta\epsilon_{l,n}(i-1,\, i)$ in the phases of the terms $(l,\, n)$, taken in different combinations, during the cycle '$i-1$' to those during the cycle 'i'.

We find the correlations between

$$S_{\text{obs}}(i) \text{ and } \sum_{n=1,3,5} \Delta\epsilon_{5,n}(i-1, i) \text{ equal to } 90\% \,,$$

$$S_{\text{obs}}(i) \text{ and } \sum_{l=1,3,5,7} \Delta\epsilon_{l,5}(i-1, i) \text{ to } 94\% \,,$$

where the combination given in the summation is the one that gives the *maximum* correlation (of the value given).

Thus, we find: (a) the size of a sunspot cycle is highly correlated to the energy *lost* by a set of waves during the current cycle, and (b) the maximum correlation is with the energy lost by the wave corresponding to the term $l = 5$ through $n = 1,\, 3,\, 5$, and also to the energy lost by the waves corresponding to the terms $l = 1,\, 3,\, 5,\, 7$ through $n = 5$.

4.5.3. *Verification of the 'Test 2'*

For verifying *Test 2* and identifying the terms of the fundamental frequency in which the energy is input, we have determined the correlations between the *changes* in the cycle size:

$$\Delta S_{\text{obs}}(i-1,\, i) = S_{\text{obs}}(i) - S_{\text{obs}}(i-1)$$

and the sums of phase shifts, in combination of terms with $n = 1$, occurring between the previous *one or two* cycles.

In the notation used earlier, the maximum correlations are:

$$\Delta S_{\text{obs}}(i-1,\, i) \quad \text{and} \quad \Delta\epsilon_{5,\,1}(i-1,\, i) : \; 87\%$$

and

$$\Delta S_{\text{obs}}(i-1,\, i) \quad \text{and} \quad \Delta\epsilon_{11,\,1}(i-2,\, i-1) : \; 90\% \,.$$

Thus the change in the cycle size from '$i-1$' to 'i' is well correlated with the amounts of energy input into the waves of frequency ν_* during the cycles '$i-2$', '$i-1$', and the maximum correlations are with energy inputs into: (a) the wave $[l = 5,\, n = 1]$ during either cycle '$i-1$' or cycle 'i' (b) the wave $[l = 11,\, n = 1]$

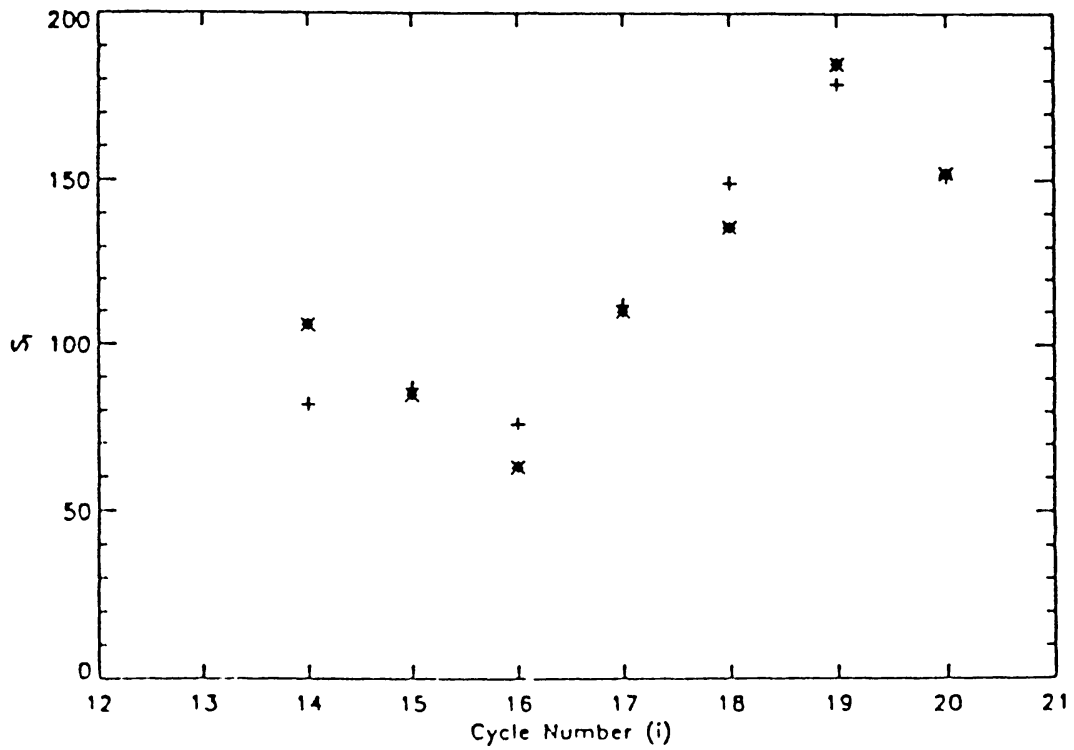

Fig. 6. The observed cycle sizes $S_{\rm obs}(i)$, represented by '+' and those 'predicted' ('$*$') on the basis of the 90% correlation of $S_{\rm obs}(i)$ to $\Delta\epsilon_{11,1}(i-2,\ i-1)$ (see Section 4.5.4).

during the cycles '$i-2$' and '$i-1$'. [*Note*: the above correlations imply that the time lapse between the input of energy and its loss through interference is longer for $l=11$ than for $l=5$. This means that the phase difference between $l=5$ and $l=11$ seen in Figure 3 should be considered as *lag* of 240° for $l=11$ rather than a lead of 120°. This is to point out that the result '(b)' need not be interpreted as energy-input in $l=11$ occurring earlier than in $l=5$.]

4.5.4. *Scope for Forecasting the 'Cycle Size'*

In Figure 6 we compare the observed cycle sizes $S_{\rm obs}(i)$ with those 'predicted' using the second correlation in Section 4.5.3. It is clear that such a forecast can be satisfactory.

5. Conclusions and Discussion

As an interpretation of the results of analysis in Sections 2, 3, and 4.1–4.2 we have suggested in Sections 4.3 and 4.4 the following phenomenological model for production of sunspot activity and maintenance of the 'approximately steady' LF spectrum of the global MHD waves.

(i) The primary input of fresh energy, into an existing spectrum of torsional MHD waves occurs mainly at $l=3,\ 5;\ \nu=\nu_*$ (by an unidentified process),

(ii) This energy cascades to the waves of higher spatial and temporal frequencies, maintaining the oscillations $B_{I,3}$, $B_{II,3}$, described in Section 3.2, and the waves of higher l, n (presumably due to reflections of the waves at the boundaries such as the photosphere and the base of the convective envelope).

(iii) The cascading energy keeps on leaking out intermittently in the form of critically buoyant toroidal flux bundles (created by superposition of waves) whose emergence produces surface fields and activity on various scales (e.g., sunspot activity from interference of waves represented by $\{l = 1, 3, \ldots, 13; n = 1, 3, 5\}$, and 'non-sunspot activity' at higher and higher l and n).

It is clear from Section 2.5 that the sunspot cycle can be modeled as arising from superposition of the LF terms in the 'rate of emergence of toroidal magnetic field', not only qualitatively in terms of the latitude-time distribution (as shown in Papers I and II), but also quantitativcly in terms of the shapes and sizes of the successive sunspot cycles.

Here the rate of emergence of magnetic field is not directly measured but is inferred from the sunspot data itself. Hence the result may appear to be a trivial consequence of the forward and the backward LF transforms. However it was seen in Paper II that the 'inferred rate' does yield the same amplitudes and phases for the LF terms, at least up to $= 13$, as those derived from the directly 'observed' poloidal flux distribution at the photosphere (Stenflo and Vogel, 1986; Stenflo, 1988). It must be noted here that on the time scales and length scales of the present model the observed photospheric poloidal field at (θ, t) will be proportional to $Q(\theta, t)$, the '*rate of emergence* of the *toroidal* flux per unit latitude interval per unit time'.

Secondly, as seen in Paper II, the behavior of the field in the *middle* (30°–60°) and *high* ($> 60°$) latitudes can be reproduced by superposition of the LF terms, though these terms were computed from the data belonging to the *low* ($\leq 30°$) latitudes.

Finally, the results in Sections 2 and 4 show that at least four groups of the LF terms in Section 3 represent real global magnetic oscillations (or waves) on the Sun.

This brings us back to the questions: (a) What is the physical nature of these waves and oscillations? And (b) What kind of steady field in the Sun's interior can sustain such oscillations ?

The answers to these questions can hardly be expected purely from a data analysis. However, for the sake of completeness of the model, on the grounds given in Sections 2.2.4 and 4.4.2 it is expected that the LF terms in 'B_Φ' represent the toroidal field component of the 'torsional MHD perturbations'. As for the question (b), we note that in a recent model of the '*steady*' part of the Sun's internal poloidal field, 'the best fit' for its *iso-rotation* with the helio-seismologically determined internal rotation of the Sun is given by terms only up to $l = 3$ (Gokhale and Hiremath, 1993; Hiremath and Gokhale, 1995). This model of the 'steady' field is constrained to an asymptotically uniform finite field at large distances and hence

can provide the necessary 'steady framework' for the oscillations. The strength of this 'steady' field (required for the '22-yr' periodicity of the torsional MHD oscillations) is $\sim 10^{-2}$ G, which would not be detectable in the presence of the periodically reversing surface fields produced by emergence of toroidal flux tubes (Sections 4.3.1 to 4.3.3). Hence the presence of the necessary 'steady' background field of primordial origin, is not ruled out.

It is also shown in the papers just referenced that the 'residuals' of the fit indicate the presence of *deviation from isorotation* (i.e., time-dependent perturbations) with $l = 5$ as the dominant term and with a time scale in the range 1–100 yr. These properties of the 'deviation from isorotation' are in agreement with the present analysis and interpretation.

The phenomenological model in Section 4.3 describes a possible way in which toroidal magnetic flux tubes could be produced. The time scales of their rise to the surface are assumed to be smaller than the smallest ($\sim$ 1 yr) resolution used in modeling the 'shapes' of the cycles. This is in accordance with the computations by Choudhury and D'Silva (1990) for radial travel of flux tubes and with the observational estimate of Howard and LaBonte (1981). However, a detailed mathematical modeling of torsional MHD waves (e.g., in a 'steady' field such as in the model mentioned above), and their interference, will be necessary for (i) ascertaining the reality of the phenomenology developed in this series of papers and for (ii) exploring the possibility of sound predictions of the 'shapes' and 'sizes' of future sunspot cycles. It will be important to model the emergence of the toroidal flux bundles, especially the separation of their identities from the ambient field and their distribution in longitudes.

The phenomenological model of the energy cascade indicates that the overall sunspot cycle phenomenon resembles a relaxation oscillation' (mentioned by Bracewell, 1988). Here the 'negative damping' corresponds to the energy input into the waves of $\nu = \nu_*$ and the 'positive damping' to the loss of energy in the form of flux tubes leaving the main body of the Sun and dissipating in the atmosphere. Therefore, the most important task will be to model the process that *perpetually excites* the waves at $\nu = \nu_*$.

At present the only mechanism of *perpetual* excitation at frequencies near ν_* which we can think of is a resonance coupling of the Sun's unstable MHD modes to the torques caused by inertial forces due to the Sun's motion about the centre of mass of the solar system. These torques will depend upon the orbital motions of the planets, whose configurations are known to have some dominant periodicities common to sunspot activity (eg. review by Seymure, Willmott, and Turner, 1992) and to the solar differential rotation (Javaraiah and Gokhale, 1994). However, the energetics of such a mechanism need to be worked out.

Acknowledgements

We thank two unknown referees for valuable comments which led to a substantial improvement in our presentation. We also thank Messrs J. S. Nathan and B. A. Varghese for their help in making the computer plots.

References

Bracewell, B. N.: 1966, *Monthly Notices Roy. Astron. Soc.* **230**, 535.
Choudhuri, A. R. and D'Silva,S.: 1990, *Astron. Astrophys.* **389**, 326.
Dziembowskii, W. A. and Goode, R. R.: 1991, *Astrophys. J.* **376**, 547.
Gokhale M. H. and Hiremath, K. M.: 1993, *Astrophys. J.* **407**, 366.
Gokhale, M. H. and Javaraiah, J.: 1990, in E. R. Priest and V. Krishan (eds.), 'Basic Plasma Processes on the Sun', *IAU Symp.* **142**, 119.
Gokhale, M. H. and Javaraiah, J.: 1992, *Solar Phys.* **138**, 399 (Paper II).
Gokhale, M. H., Javaraiah, J., Kutty, K. N., and Verghese, B.: 1992, *Solar Phys.* **138**, 35 (Paper I).
Hiremath, K. M. and Gokhale, M. H.: 1995, *Astrophys. J.*, submitted.
Howard, R. and LaBonte, B. J.: 1981, *Solar Phys.* **74**, 131.
Javaraiah, J. and Gokhale, M. H.: 1994, *Solar Phys.*, submitted.
LaBonte, J. and Howard, R.: 1982, *Solar Phys.* **75**, 161.
Mestel , L. and Weiss, N. O.: 1987, *Monthly Notices Roy. Astron. Soc.* **226**, 123.
Spruit, H. C.: 1990, in G. Berthomiu and M. Crivier (eds.), *Inside the Sun*, Kluwer Academic Publ., Dordrecht, Holland, p. 415.
Stenflo, J.: 1988, *Astrophys. Space Sci.* **144**, 321.
Stenflo, J. and Vogel, M.: 1986, *Nature* **319**, 285.
Seymore, P. A. H., Willmott, M., and Turner, A.: 1992, *Vistas Astro.* **35**, 39.